A TWO-DIMENSION POSITION SENSITIVE HIGH EFFICIENCY TRANSITION RADIATION DETECTOR FOR HIGH COUNTING RATE ENVIRONMENT

M.PETROVICI[1], V.SIMION[1], M.PETRIŞ[1], V.APRODU[1], D.BARTOŞ[1], G.CARAGHEORGHEOPOL[1], V.CĂTĂNESCU[1], A.HERGHELEGIU[1], L.PRODAN[1], A.RADU[1], C.BERGMANN[2], M.KLEIN-BÖSING[2], J.P.WESSELS[2]

[1]Horia Hulubei National Institute for Physics and Nuclear Engineering, Bucharest-Magurele, P.O.Box MG-6, RO-077125, Romania
E-mail: mpetris@ifin.nipne.ro
[2]University of Münster, Germany

Received June 22, 2010

A two-dimension position sensitive Transition Radiation Detector (TRD) was designed, built and tested. The prototype consists of two individual multiwire proportional chambers (MWPC) that share a thin common central readout electrode. The rectangular pads of the previous prototypes [1] were split on diagonal for position determination in both coordinates: across and along the pads, respectively. Measurements with X-ray sources showed a very good energy and position resolutions. These results open the possibility of constructing large TRD arrays for high counting rate experiments with a reasonable number of layers and very good two-dimension position information.

1. INTRODUCTION

The Transition Radiation Detector (TRD) architecture proposed by us [1]– [3] for lepton identification with the CBM experiment [4] at the future FAIR facility at GSI [5] is based on a double sided pad structure read-out electrode. Electron-pion discrimination efficiency better than 1% for a six layers configuration [1] and position resolution of the order of 160 μm [3] up to an average particle rate of $2{\cdot}10^5$ particles$\cdot$cm$^{-2}\cdot$s^{-1} were achieved.

The active area of the prototypes developed up to now, i.e. 4.5 x 2.0 cm^2, is too small to provide a reasonable geometrical efficiency for an large array based on such cells. Therefore, a larger size prototype, using the same architecture, had to be developed. This can be achieved by increasing the sizes of the rectangular pads of the central double sided read-out electrode. Obviously, this conflicts with the requirements of high granularity and position resolution. In order to cope with this, we split on diagonal the rectangular pads of the read-out electrode.

This paper presents the results obtained in testing such an architecture using radioactive X-ray sources. The next chapter describes the construction scheme of the detector. Chapter 3 gives information on the experimental setup used in tests

performed with radioactive X-ray sources ^{55}Fe and ^{238}Pu. Experimental results in terms of energy and two dimension position resolutions are presented in Chapter 4. Chapter 5 is dedicated to the conclusions.

2. DETECTOR GEOMETRY

The structure of the detector can be followed in Fig. 1. The central readout electrode separates the detector into two identical sections. It has a pad structure on both sides; the corresponding pads on the upper and lower surface are connected. Each rectangular pad of 10 x 80 mm^2 is split on diagonal, each triangle being readout separetely. The choice of triangular-pad geometry allows for position determination in both coordinates: across and along the pads, respectively. The two anode planes,

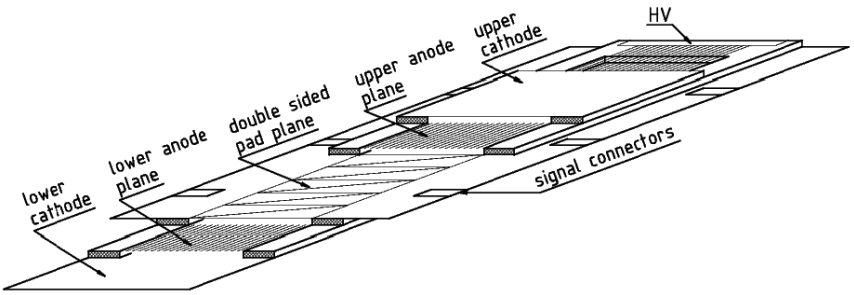

Fig. 1 – Schematic view of the detector structure.

up and down relative to the central electrode, are made from gold plated tungsten wires of 20 μm diameter with an anode wire pitch of 3.0 mm. Aluminized kapton foil (25 μm) glued on a Rohacell plate is used to close the gas volumes providing at the same time the outer cathodes of the respective MWPCs. The anode-cathode distance is 3 mm. A photo of the inner structure before closing it with the gas windows (outer cathodes) can be seen in the left panel of Fig.2. One could follow the geometry of the pads on the central electrode and the anode wires running across the pads. The readout electrode has 72 triangular pads, 36 read-out on the left-side and 36 on the right-side of the counter.

Two versions of such a detector were built. One chamber was built with the central readout electrode made from a PCB (Printed Circuit Board) of 300 μm thickness to test the basic functionality of the design. The second version of the prototype has an identical structure with the first one. In this case, the central readout electrode was made from a kapton foil of 25 μm on which, by etching the Cr (20 nm) and Al (200 nm) layers deposited by evaporation on the kapton support, on both sides was obtained the pad structure.

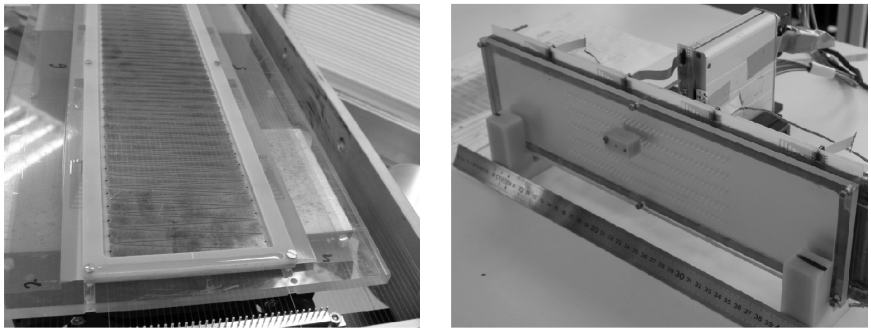

Fig. 2 – Left panel: a photograph of the internal structure before mounting the gas foils. Right panel: a photograph of the experimental set-up used for X-ray source tests.

3. EXPERIMENTAL SETUP FOR TESTS USING X-RAY RADIOACTIVE SOURCES

The experimental setup is shown in the right side of Fig.2. A custom built

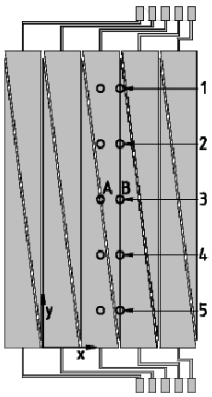

Fig. 3 – The position of collimators relative to the central electrode pads.

8 channel charge-sensitive preamplifier/shaper (2mV/fC gain; 1800 electrons rms noise) was used to process the signals of 8 triangular pads, digitized by an AD811 peak sensing ADC. The anode signal was processed by a low noise charge sensitive preamplifier and a spectroscopy amplifier with a 2 μs shaping time, (designed in NIPNE-HH, Bucharest for high performance gamma ray spectoscopy).

The source was carefully collimated using two columns of five collimators as it is shown in Fig. 3. The x direction is parallel with the anode wires (across the pad) and the y direction is perpendicular on the anode wires (along the pad) as can be followed in Fig. 3. Column A is on the center of a rectangular pad and column B is centered on the border line between two adjacent rectangular pads, the relative distance between the two rows being 5.25 mm. Each collimator has a diameter of 2

mm. Along y direction the collimators were distributed equidistant, 12 mm appart, with the middle collimator centered on the counter.

The MBS GSI-type data acquisition system has been used [6]. A 2 l/h flow of Ar/CO_2(70%/30%) gas mixture was circulated through the counter at atmospheric pressure.

4. RESULTS

4.1. ENERGY RESOLUTION USING ^{55}FE X-RAY SOURCE

Typical amplitude (energy) spectra obtained in ^{55}Fe source tests for the first

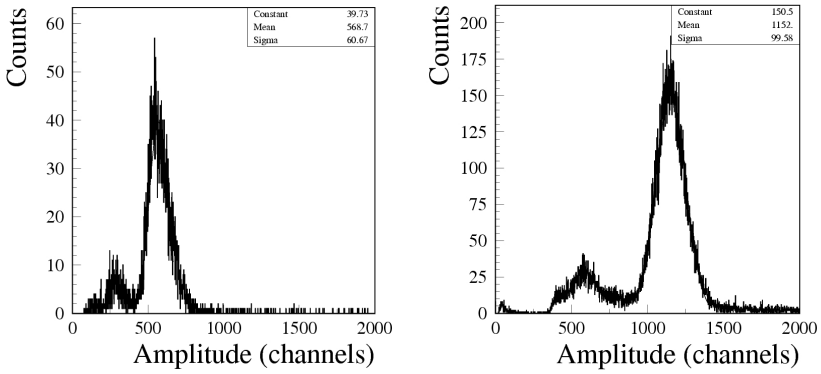

Fig. 4 – The pulse height spectra of a ^{55}Fe source taking the signal from anode wires (left)and from the pad plane readout electrode (right) at 1750 V anode voltage.

version of the prototype, using anode signal (Fig. 4 - left panel) and pad plane signal (Fig. 4 - right panel), respectively, showed very good energy resolution. In the case of pad plane readout, the signals of six consecutive triangular pads (3 rectangular pads, with the central one having the largest signal) were summed-up.

4.2. POSITION RESOLUTION USING ^{238}PU X-RAY SOURCE

As it is known, the coordinate reconstruction and the position resolution performance depend on the charge spread over the pads. This was estimated based on the parametrization of induced charge density on rectangular pads [7].

$$\sigma(d) = -\frac{Q}{2\pi}\Sigma_{n=0}^{\infty}(-1)^n \frac{\lambda_n}{[\lambda_n^2 + d^2]^{3/2}} , \qquad \lambda_n = (2n+1)l \tag{1}$$

where l is the anode-cathode distance, d is the distance from the center of the avalanche at a point (x,y) on the readout electrode plane, Q is the charge generated by the

avalanche on the anode wire.

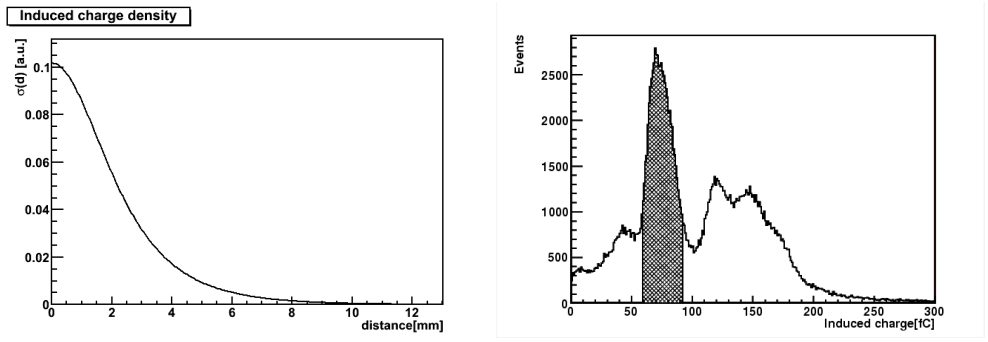

Fig. 5 – Left side: induced charge density on the cathode plane as a function of distance to the center of the avalanche, corresponding to the geometry of our prototype, based on the parametrization given by Eq.1. Right side: calibrated charge distribution obtained using ^{238}Pu source and an anode high voltage of U$_a$ = 1800 V.

The induced charge density distribution for our specific configuration can be followed in Fig. 5 - left side. Already from this representation it becomes clear that, as a function of the position of the avalanche, there are situations when only mainly two pads have signals. As far as our ^{55}Fe source was very weak to be collimated, all tests for position resolution studies were performed using a ^{238}Pu source with higher intensity which excited also the characteristic 8.0 keV Cu X-ray line from the PCB central electrode. The Fig. 5 - right panel shows the callibrated induced charge

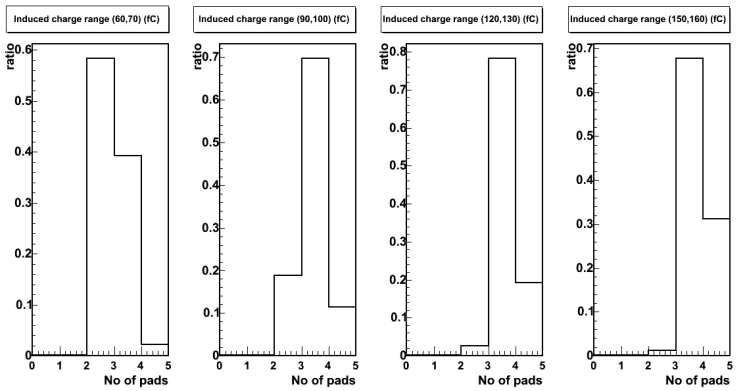

Fig. 6 – Distributions of number of rectangular pads fired for different windows of induced charge values for a fixed anode voltage of U_a = 1800 V.

spectrum obtained using ^{238}Pu source for an applied anode voltage U_a = 1800 V. The hachured area correspons to the Cu characteristic 8.0 keV line.

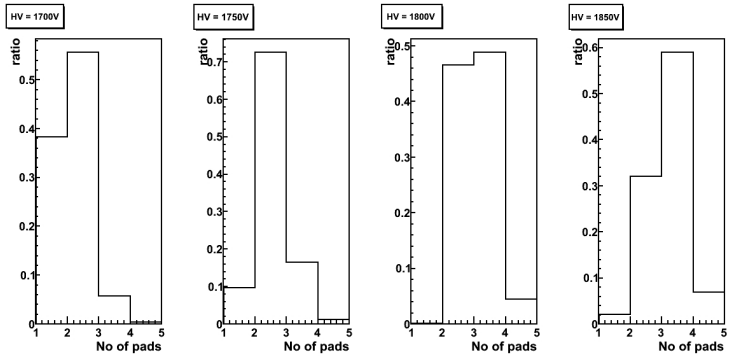

Fig. 7 – Distributions of number of rectangular pads fired for different anode voltages with a selection of the events corresponding of the hachured peak of induced charge distribution (Fig. 5 - right panel).

The distribution of number of rectangular fired pads in a single event, for different charge windows taken in the mentioned distribution, when the source was positioned on the central collimator of column A, is presented in Fig.6. The induced charge on each pad was determined after subtraction of ADC pedestals and gain correction for amplifiers and ADCs. Hence, within these conditions, the pad cluster was derived requiring the pad charges to be positive. As one could see, bellow 120 fC (the average induced charge on the readout electrode by a minimum ionizing particle), the number of events where only two rectangular pads are fired is significant. Similar studies were performed for different anode voltages, with a selection of the events corresponding of the hachured peak of induced charge distribution from Fig. 5 - right panel. The obtained results are presented in Fig. 7.

For U_a = 1750 V and taking only events in which at least three rectangular pads were fired the position resolution in x direction was determined. The position was reconstructed considering a cluster of three rectangular pads (the pad with maximum signal and its left-right neighbours). The pulse height information of each pad, positioned at the respective geometric centroid of the pad, was fitted with a Gauss function for x coordinate reconstruction. The results can be followed in Fig. 8, upper and bottom rows corresponding to the group A and group B, respectively of collimators. The second peak seen in each distribution is due to the X-rays that penetrate the thin plexiglass wall between two rows of collimators. An average standard deviation of $\sigma_x \sim 1.34$ mm is obtained from the fits. For the used collimator diameter of 2 mm, a corresponding spot size of ~ 3.2 mm on the anode plane is expected. If we substract the spot size contribution, an intrinsic position resolution of $\sigma_x \sim 0.970$ mm is obtained. For position information across the anode wires (y coordinate) we used the intersection of two lines, each one parallel with the y coordinate in two coordinate systems: one associated to the rectangular pairing of triangular pads (x, y) and the other one corresponding to the tilted pairing ($x^{'}$, $y^{'}$, with $y^{'}$ direction paralell with

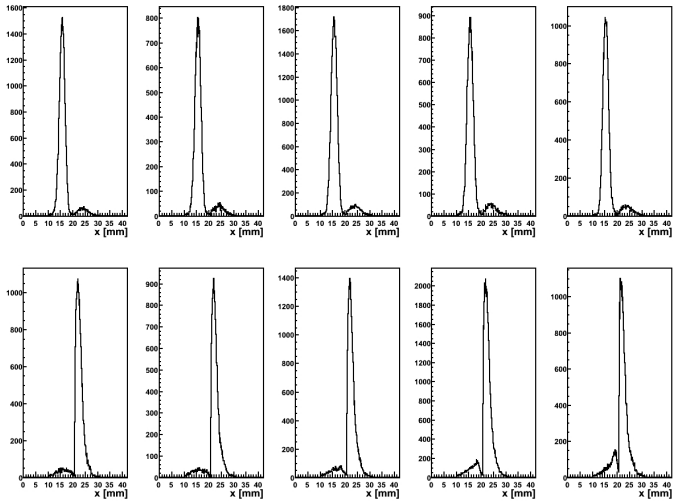

Fig. 8 – Position resolution in coordinate x - across the rectangular pads for U_a = 1750 V and taking only events in which at least three rectangular pads were fired. Upper row for group A of collimators, bottom row for group B of collimators.

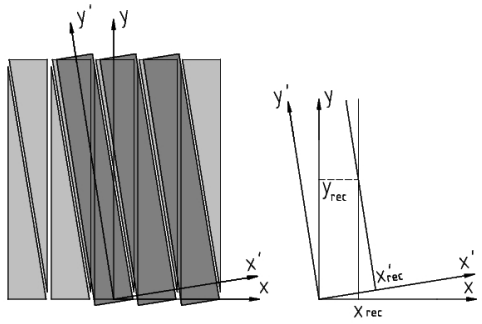

Fig. 9 – Description of the method used for the position information along the rectangular pads (across the anode wires).

the diagonal of a rectangular pad) as it is schematically represented in Fig. 9. The results can be followed in Fig. 10, upper and bottom rows corresponding to the group A and group B, respectively of collimators. An average standard deviation of $\sigma_y \sim$ 2.49 mm is obtained from Gauss fits of the presented distributions. Subtracting the contribution of the spot size estimated on the anode plane, an intrinsic y resolution of $\sigma_y \sim 2.31$ mm is determined.

One should remember that these results were obtained for the events in which at least three rectangular pads were fired. We should, however, take the full advantage of the split pad architecture. The upper row of Fig. 11 shows the distribution of

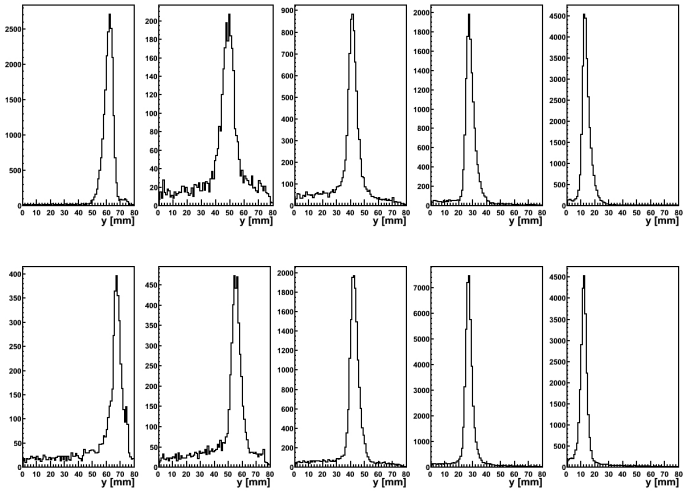

Fig. 10 – Position resolution in coordinate y - along the rectangular pads for U_a = 1750 V and taking only events in which at least three rectangular pads were fired. Upper row for group A of collimators, bottom row for group B of collimators.

the number of fired triangular pads for different values of induced charge for an anode voltage of U_a = 1800 V. One can see that this number increases from four for low induced charge to six for the high values of the induced charge. The bottom row shows the same distribution as a function of anode voltage for a window in the induced charge distribution obtained with the ^{238}Pu source corresponding to the hachured peak. The number of triangular pads with signal increases from three at the lowest voltage to five at 1800 V anode voltage. For the position reconstruction with triangular pads we need at least four such pads fired in an event. In order to make use of this information a procedure based on a two dimensional pad response function for extracting the position information in xy plane is under development.

It is well known that one of the important factors affecting charge sharing among the pads are the geometrical parameters. Hence, an improvement can be obtained either by decreasing the width of the pads or by a slight increase of the gap between the electrodes. Plots of the induced charge on the pad plane as a fuction of the distance to the avalanche for three values of the anode-cathode distance are presented in Fig. 12. An improvement of the charge sharing by about 1.3 in FWHM going from a gap of 3 mm to a gap of 4 mm could be observed. This is the reason for which the third version of the prototype will be built having 4 mm anode-cathode distance.

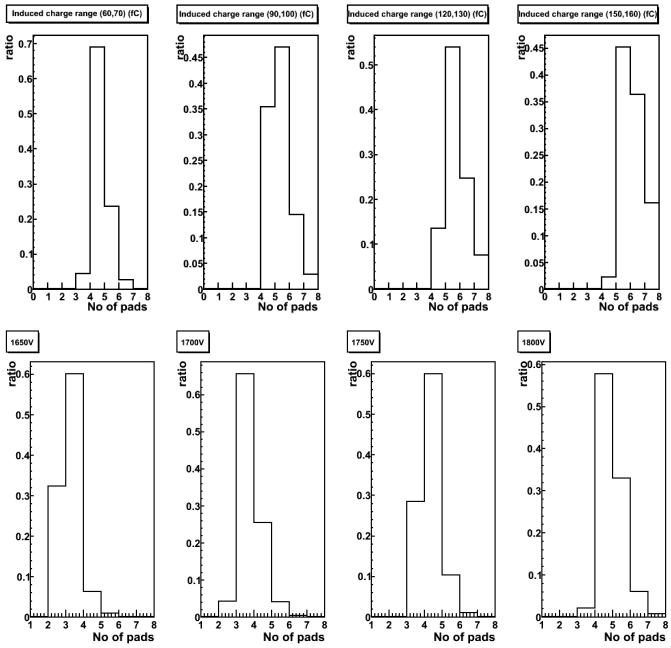

Fig. 11 – Upper row-distributions of number of triangular pads fired for different windows of ^{238}Pu induced charge distribution for an anode voltage of U_a = 1800 V.Bottom row - distributions of number of triangular pads fired for different anode voltages and a window in the induced charge distribution (Fig. 5 - right panel) corresponding to the hachured peak.

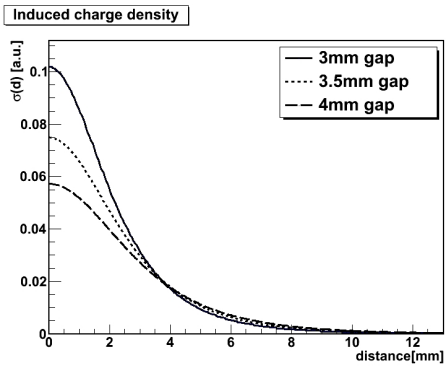

Fig. 12 – Induced charge density on the cathode plane as a function of distance to the avalanche, corresponding to different anode-to-cathode distance.

5. CONCLUSIONS

For electron-pion discrimination in high counting rate environment a new TRD prototype based on a two-dimention position sensitive, double sided pad read-out electrode was designed, built and tested. First results on the detector performance using radioactive X-ray sources have been presented in this paper.

The prototype shows a very good performance in terms of energy and position resolution. Detailed in-beam investigation for electron-pion discrimination capability and high counting rate environment performance will be done in the near future. However, based on our previous results [1], as far as the distance between the electrodes remained the same, the same electron-pion rejection efficiency is expected as a function of counting rate. All these recommend this principle of double sided two-dimentional position sensitive TRD as a solution for high counting rate environment TRDs with reduced number of channels and material budget, for a given electron-pion discrimination performance.

Acknowledgements. This work was supported by CAPACITATI/Modul III, contract no. 42EU and PARTENERIATE contract no. 71-144 financed by the Romanian National Authority for Scientific Research and WP18-Hadron Physics2/FP7 contract no. 227431 financed by EU.

REFERENCES

1. M. Petrovici *et al.*, Nucl. Instr. and Meth. **579**, 961 (2007).
2. M. Petriş *et al.*, Nucl. Instr. and Meth. **581**, 406 (2007).
3. M. Klein-Bösing *et al.*, Nucl. Instr. and Meth. **585**, 83 (2008).
4. CBM - *Technical Status Report*, 2005.
5. *FAIR Baseline Technical Report*, http://www.gsi.de/fair/report/btr.html.
6. H.G. Essel and N. Kurz, GSI Ann. Rep. 1998, 188.
7. M. Benayoun *et al.*, Nucl. Instr. and Meth. **342**, 483 (1994).